REDUCTION OF ERRORS CAUSED BY CROSS-POLARIZATION IN A MICROSTRIP ANTENNA

ASEDA SARAH (BEd. Sc)

REG. NO.: I56/20404/12

A Thesis submitted in partial fulfilment of the requirements for the award of degree of Master of Science (Electronics and Instrumentation) in the School of Pure and Applied Sciences of Kenyatta University

JANUARY 2020

DECLARATION

I declare that this thesis is my original work and has not been presented for a degree or any other award in any other university.

Aseda Sarah (B Ed Sc.) Signature …….....Date……

REG. No.I56/20404/2012

This thesis has been submitted with our approval as the university supervisors

Dr. Mathew K. Munji Signature…… .....Date……

Department of Physics

Kenyatta University

Dr. Kibet Langat Signature …….....Date……..

Department of Telecommunication and Information Engineering

Jomo Kenyatta University College of Agriculture and Technology

ACKNOWLEDGEMENTS

The success of this work was achieved through valuable contribution from other people.

I therefore gratefully acknowledge my dedicated supervisors Dr. Matthew Munji and Dr. Kibet Langat for their guidance and advice at all stages of my work. The entire work was made possible by the reading, correction and fruitful discussion of my entire work.

Many thanks go to the technical staff at the University of Nairobi Telecommunication department. In particular I would like to thank the telecommunications technicians Mr. Boniface Munyole and Mr. Edwin Rotich for their assistance during the fabrication and the testing stages of my research work.

I acknowledge with gratefulness my dear brother Engineer Ken O. Aseda and his family who provided a favourable working environment for my research work. They also provided technical and moral support.

My sincere thanks go to my loving husband Richard who ensured that I pursued my dream through encouragement, comfort and financial assistance throughout my studies. He also enabled my successful travel for my project work.

Finally, I thank God for life and good health during this entire period.

DEDICATION

To my only children, Rene Loch, Ray Lwanda, Rheba Lwasi, Raniella Lulu and aspiring future Women scientists. May this work be an inspiration to you all as you develop your future career.

TABLE OF CONTENTS

CHAPTER THREE

MATERIALS AND METHODS

CHAPTER FOUR

RESULTS AND DISCUSSION

LIST OF FIGURES

LIST OF TABLES

LIST OF SYMBOLS

Br – bromine

dB- decibels

dBi- decibel- isotropic

dBm- decibel milliwatt

^{o}c - degree celcius

ε_{r} – relative dielectric constant

δ – Loss tangent

λ – Wavelength

Ω - Ohm

f_r - resonant frequency

f_o - fundamental frequency

g/cm^3 – grams per cubic centimetre

GHz- gigahertz

Hz – Hertz

ln – natural log

MV/m – megavolt per metre

OH – Hyroxyl ion

CH – Carbon Hydrogen

X_f – probe position along the x-axis

Y_f – probe position along the y-axis

LIST OF ABBREVIATIONS AND ACRONYMS

CAD	Computer Aided Design
CMPA	Concentric Microstrip Patch Antenna
CPA	Circular Patch Antenna
EM	Electro-magnetic
EMCoS	Electromagnetic Compatibility Software
FEM	Finite Element Method
FR-4	Flame Retardant 4/Fibre glass Resin 4
GSM	Global System for Mobile Communication
GPS	Global Positioning System
HFSS	High Frequency Structure Simulator
IE3D	Integrated Electromagnetic in 3-Dimensions
MPA	Microstrip Patch Antenna
MSA	Microstrip Antenna
NEC	Numerical Electromagnetic Code
PCB	Printed Circuit Board
RL	Return Loss
SMA	Sub Miniature version A
SNA	Scalar Network Analyzer
TLM	Transmission Line Model
TE	Transverse Electric
TEM	Transverse Electric Magnetic
TM	Transverse Magnetic

VSWR	Voltage Standing Wave Ratio
VL	Virtual Lab
WIFI	Wireless Fidelity
WLAN	Wireless Local Area Network
WSN	Wireless Sensor Network

ABSTRACT

Microstrip antennas are used for transmitting and receiving electromagnetic signals. The transmitted signals can be reflected back within the building. This affects the strength of signal transmission. Polarization of the electric field determines the signal strength of the electromagnetic wave. If cross polarization occurs then it results in multiple signals which interfere with each other causing some signal loss during transmission. The main focus of the study was to reduce cross polarization in a microstrip antenna. The study involved designing a circular patch antenna (CPA) and Concentric microstrip patch antenna (CMPA) with an annular patch enclosing the circular patch. Simulation and optimization was also done using Ansoft high frequency structure simulator (HFSS). The antenna was then fabricated using photolithography method using the optimized radii. The results obtained during simulation and fabrication process were then analysed and evaluated. During optimization, the initial radius of the circular patch and the width of the annular patch were varied to match the required frequency of 2.4GHz. The antennas were fed using a single coaxial probe towards the centre of the circular patch. The antenna characteristics like the radiation efficiency, directivity, gain, return loss (RL) and the radiation patterns were studied using HFSS software and the patch size optimized to obtain the best results. The analysis and testing of the fabricated antenna was done using a Scalar Network Analyzer (SNA). The RL in decibels (dB) was studied to show the effect of cross polarization on a CPA and the Concentric Microstrip Patch Antenna (CMPA). In Ansoft HFSS, the circular patch had a gain of 1.8147 and directivity of 4.1753 while the circular patch with annular had a gain of 2.3354 and directivity of 5.3212. The simulated data showed a performance improvement of 29% for the gain, 27% for the directivity and 11% for RL. A study of the radiation patterns of the two designs showed reduced cross-polarization in the performance of the antenna with an annular patch around it. The RL of the fabricated antenna; CPA and CMPA were studied using the SNA. The experimental circular patch had a Return loss of -9.697dB and the CMPA had a Return Loss of -13.170 dB. The experimental CMPA reduced cross polarization by 35.8% as compared to the fabricated CPA. The research has therefore proved that an annual ring can be used as a polarization filter to reduce cross polarization errors of signals transmitted by a circular patch antenna. The experimental CMPA gave the best performance in error reduction as compared to the CPA. The results obtained show that cross polarisation can be reduced by removing some metal on the surface of a circular patch antenna and the size of the antenna should be reduced as much as possible to enable it fit in handheld devices.

CHAPTER ONE

INTRODUCTION

Microstrip patch antennas are used to transmit and receive electromagnetic waves using a radiating patch separated from a ground plane by a dielectric material. Many studies have been done on microstrip patch antennas. The study of circularly polarized microstrip antenna has also been investigated by other scientists showing that signal transmission losses can be reduced by circular polarization.

1.1 Background

An antenna is a device which can radiate and receive electromagnetic (EM) energy in an efficient and desired manner (Huang and Boyle, 2008). Cross polarization occurs on the signals transmitted by an antenna. These signals interfere with each other during transmission causing errors on the strength of their transmission. Wireless systems transmit electromagnetic signals using antennas. Microstrip antennas (MSAs) consist of a radiating patch on one side of a dielectric substrate which has a ground plane on the lower side as shown in Figure 1.1.

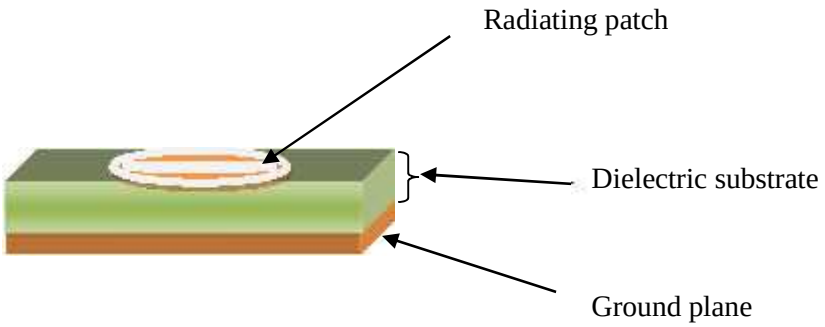

Figure 1.1: Simple diagram of a microstrip antenna

Practical microstrip radiators were fabricated earlier for use in antenna systems (Howell and Munson, 1974). The MSAs uses a Printed Circuit Board (PCB) technique. The PCB has an insulated dielectric separating the radiating patch and the ground plane. It provides electrical

connection between the points to be interconnected and should be reduced in size for better performance and reliability. In this study, a Circular Patch Antenna (CPA) consists of a circular patch with a coaxial probe near the centre on an FR4 substrate while a Concentric Microstrip Patch Antenna (CMPA) consists of a centrally located and probed circular patch with an annular patch around it on an FR4 substrate.

1.2 Radiation mechanism

A patch antenna is a voltage radiator (Puthanial and Kishore Raja, 2016). Radiation is determined by the field distribution between the patch and the ground plane. The patch on a microstrip antenna is made up of a conducting material like copper. The fringing field between the patch edge and the ground plane causes radiations on an MSA. Figure 1.2 is an illustration showing that when the patch is connected to a power source, it has a charge distribution on the upper side and the lower surface of the ground plane (Lavado, 2009). A patch is half a wavelength long at its dominant mode. This theoretical study ruled out the helix and conformal antenna due to their narrow bandwidths 2 MHz and found results of RL ≤ - 10dB and Axial Ratio ≤ 3dB. Repulsive force between the positive charges create a charge density around the edges while attractive forces between the unlike charges cause most of the current and charge concentration to remain underneath the patch (Lavado, 2009).

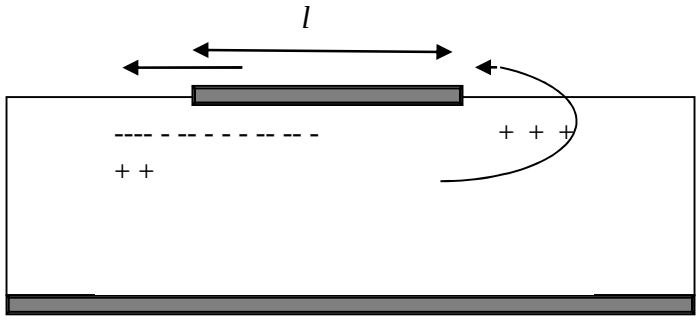

Figure 1.2: Showing distribution of charge

1.3 Polarization

Polarization takes place during transmission of signals. Polarization is the orientation of the electric field vector or magnetic field vector in relation to the direction of propagation of the electromagnetic wave. Polarization can either be linear or circular. Linear polarization occurs if the electric field vector or magnetic field vector travel in the same direction as the direction of propagated wave. In circular polarization, the electric field vector rotates perpendicularly around the direction of propagation with a constant magnitude. Circular polarization occurs if the electric and magnetic field vectors for the transmitted wave have two orthogonal linear components with the same magnitude and the time phase difference is an odd multiple of 90^{o} (Edling, 2012). A circular MPA (Microstrip Patch Antenna) is also good for circular and linear polarization. An annular patch occupies a smaller physical space. Removing some metallic surface around the circular patch creates a circular patch surrounded by an annular patch around it. Multiple paths of signals may be caused by radiations being reflected by the surrounding surfaces like walls and reflecting surfaces resulting to cross-polarization. Cross-polarization occurs when destructive interference occurs between the transmitted and the reflected electromagnetic wave.

1.4 Problem Statement and Justification

Cross polarization results in interference of transmitted signals which result to weakening of signal strength. The interference between the transmitted and reflected wave is destructive in cross polarization. This effect is reduced in a circular patch since it produces waves which are circularly polarized. In this study, an investigation into the designs of a circular patch antenna (CPA) by adding an annular patch antenna. Low cross polarization enables most of the transmitted signals to be directed towards the receiving antenna therefore reducing losses.

Multiple reflections are experienced within most buildings when using handheld devices like mobile phones. This causes cross polarization which lowers the radiation efficiency of the transmitted signals. An annular patch used also helps in reducing the size of the patch antenna.

1.5 Objectives

1.5.1 General Objective

To reduce cross polarization effects in a microstrip antenna.

1.5.2 Specific Objectives

i. To design a CPA with varied radius and CMPA with varied width of the patches using Ansoft HFSS software.
ii. To simulate a CPA and CMPA using Ansoft HFSS software for optimized radii.
iii. To fabricate a CPA and CMPA consisting of an outer annular ring patch enclosing a centrally located circular MSA using the optimized results.
iv. To evaluate the performance of the CPA and CMPA using the simulated and experimental results.

1.6 Rationale

Cross polarization errors can be reduced by a well designed circular patch antenna with an annular patch around it. Studies have shown that removing metal around the circular patch results to a ring around it which helps in extending the surface of the radiating patch due to fringing effect. This increases the electrical size of the patch. The circular patch and the annular patch have been studied on other frequencies with back lobes. Many studies on the CPA indicate designs and simulation with back lobes which confirms interference of transmitted signals. In previous studies, perturbations have been used to reduce cross polarization on the ground plane

and the surface patch. For this study, the ground plane is not interfered with but the surface circular patch has a ring around it. This study also involves fabrication of a CPA having an annular patch around it. The annular patch is used as a signal reflector since it is an auxiliary element. The annular patch's effect on the radiated signals strength is studied.

CHAPTER TWO

LITERATURE REVIEW

This chapter contains a review of some studies on polarization, the design of the microstrip antenna, patch geometry and the feed network.

2.1 Polarization

Polarization can be linear or circular depending on the patch geometry. This section involves studies of these two types of polarization used in this research and their effects in radiation of signals. In linear polarization, the EM field is broadcasted in a plane normal to the direction of propagation. Circular polarization has its EM fields rotating around the line of propagation and at 90^{o} phase difference from each other. Cross polarization occurs when the reflected electromagnetic wave is perpendicular to the radiated or received wave (Ramesh *et al*., 2001). If antenna polarization is perpendicular to the field of polarization, then it produces low power. Polarization in a circular disk is linear unless metallization is removed around it to form a circular patch creating a good condition for circular polarization (Kerr, 1978). A theoretical investigation on microstrip ring antenna with good isolation at 1.8 GHz using cavity model was conducted. A study of the "cross-polarization of spherical-circular microstrip patch antenna" concluded that in TM_{11} mode, a small radius reduces cross polarization of a circular patch antenna (Chen and Wong, 2007). Marwa (2010) carried out an investigation on "Circularly polarized microstrip antenna" which involved designing a single fed circularly polarized MSA. Marwa further reported that circular polarization reduces the effect of multipath reflection. Ground plane diffraction effect contributing to the back lobes can be reduced using resistivity tapered ground plane (Rao *et al.*, 2012). A single layered rectangular MSA with corrugation like

defects to reduce cross-polarization was also studied. The design was done on FR-4 substrate and the peak gain was 5 dBi (decibel in isotropic antenna) at frequency of 7.72 GHz. The corrugation like defects improved polarization parity over a wide range (Pawar *et al*., 2018). Hansen (1987) studied cross polarization characteristics of circular and rectangular patches by looking at peak value angles. Hansen concluded that the peak value angles depended on the substrate's dielectric constant and the patch thickness. Rectangular patches were found to have little effect. Chattopadhyay and Chakraborty (2018) studied cross polarization radiation of a rectangular microstrip patch antenna at a lower order dominant mode of TM_{10}. The nature of the field beneath the patch was found to contribute to cross polarization. They proposed a T-shaped microstrip antenna to suppress the cross-polarization of the rectangular patch from a theoretical discussion.

2.2 Microstrip antenna design

In designing a MSA, it is important to study its radiation mechanism and patch geometry. Different design methods have been used in reducing multipath signal interference in MSAs.

2.2.1 Patch Geometry

The design of the patch contributes a lot in reducing cross-polarization in MSAs. There have been several studies on the geometries of the top conducting surface of MSA designs like square, rectangular, circular and triangular patches. Mutiara *et al.* (2011) designed a rectangular microstrip patch antenna radiating at a frequency of 2.4 GHz on a syrofoam dielectric substrate (ε_r =1.03). This antenna was fed through a coaxial probe and design simulated using superNEC (Numerical Electromagnetic Code) and 4NEC2X giving a gain of 11 dB outdoor place and 15 dB indoor place. On testing the MSA, it could be used as a client antenna in computers and workable antenna for wireless fidelity (WIFI). Tecpoyotl *et al.* (2012) investigated a circular,

rectangular and pentagonal annular geometries and their effect on bandwidth of antenna arrays using RT/Duroid 5880 substrate. They concluded that the bandwidth of the antenna depends on the width of the external ring and location of the feed point. Sharma *et al.* (2012) investigated the design of a circular probe-fed MSA on a glass epoxy. Simulation was done using the Integrated Elecromagnetic in 3-Dimensions (IE3D) software based on the cavity model at a frequency range from 2.7 GHz - 2.9 GHz and the value of the return Loss decreased to -26.65 dB from -14.4 dB as the radius of the antenna increased. The voltage standing wave ratio (VSWR) showed a high reflection coefficient because the simulated results reduced from 1.47 to 1.098 as radius increased from 14.80mm to 14.85mm at a resonant frequency of 2.8 GHz. The measured value gave a RL of -10.94 dB and a VSWR of 1.792.

Wang *et al*. (2012) designed, optimized and fabricated a compact annular ring MSA for wireless systems network at 2.4 GHz. Ansoft HFSS was used in the simulation. The MSA had a Steel installation base-Chip resistor at 120_{Ω} giving a good radiation pattern with low cross polarization, RL = -34.2 dB and Peak gain = 2.5 dBi. Kumar *et al.* (2013) designed a rectangular microstrip patch antenna for 2.4 GHz wireless application using Ansoft HFSS on flame retardant (FR4) substrate. It had a RL = -38 dB, gain = 3.95 dB, mismatch loss = 0.042 dB. Singh *et al.* (2013) designed and analysed an annular ring slot MSA for wireless UHF applications using IE3D software which showed that the annular ring slot MSA offers a better bandwidth as compared to other conventional shapes of the patch. Kamal *et al.* (2014) used FR4 substrate to design a circularly polarized MSA for wireless applications operating at a frequency range of 1.9 GHz -2.5 GHz and axial ratio was below 3 dB. Ingale *et al*. (2015) used Ansoft HFSS to simulate a rectangular microstrip patch antenna at frequency of 2.34 GHz using RT/ Duroid and FR4 substrates. FR4 substrate had better results of RL = -24.15 dB, gain = 3.92 dBi, bandwidth=

67 MHz and VSWR< 2. Gupta and Singh (2015) designed an annular ring MSA for dual band operation in the frequency range of 4.5 GHz – 9.2 GHz. They did a simulation using IE3D electromagnetic simulation which gave good directivity with a RL < -19 dB and VSWR < 1.5. Puthanial and Kishore (2016) simulated and analysed a rectangular patch antenna using AN-SOF Professional V 3.5. They compared the patch antenna at a frequency of 2.4 GHz and 18 GHz on RT Duroid dielectric. They concluded that the 18 GHz offered a better RL = -14 dB and gain = 6 dB while 2.4 GHz offered a RL= 0.087dB and gain = 5 dB.

2.2.2 Feed network

The antenna's feed technique affects its polarization characteristics. The methods can be line feed, probe feed or aperture feed. In coaxial probe, there are three components: the conductor at the centre, the dielectric material and a coaxial cable shield as shown in Figure 2.1. A 50 Ohm coaxial cable is the most appropriate to use for high power handling and low attenuation characteristics. The impedance of 50 Ohms is a measure of resistance by the alternating electric current.

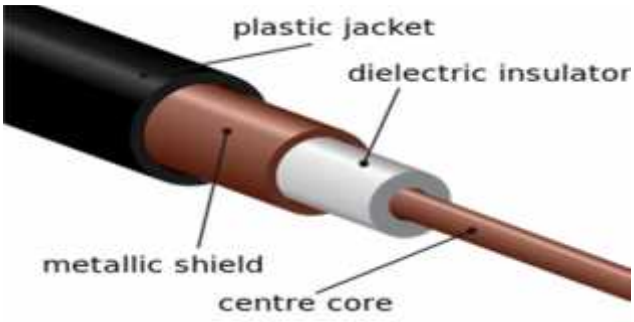

Figure 2.1: Parts of a coaxial cable

It was concluded that surface waves and feed line configurations were probable sources of cross-polarization radiation in the study of the cross-polarization factors affecting arrays (James and Hall, 1989). The width of the external ring, gap length and location of the feed network affects

the radiation pattern of the antenna (Tecpoyotl *et al.,* 2012). To obtain a single fundamental frequency with two radiating elements, a single feed line is required on one element as the reference element (Hiroyuki and Yingcheng, 2011). The probe geometry of a low cost MSA is not suitable when antennas are arranged in series in an assembly line (Nascimento and Lacava, 2011). A dual orthogonal feeding and perturbation also results to circular polarization (Lavado, 2009). A study on the effect of the feed location on the performance of a circular patch MSA by Mom, *et al*. (2013) concluded that a lower RL = -37.04 dB was obtained with the feed towards the centre of the circular patch at 5mm left of the centre. Therefore, the feed location should be as closer to the centre of the circular patch as possible in order to reduce losses during transmission.

2.3 Summary on Literature Review

The studies above proved that the circular patch offered a better radiation performance as compared to the other geometries. A combination of a probe-fed circular patch with an annular patch resulted to a small, thin MSA with reduces cross polarization effects. Most of the previous research was mainly on design and simulations. The line feed network also contributed more to cross polarization as compared to the coaxial probe. Very few fabrications were done by previous researchers. Therefore, this research incorporates previous studies involving circular, annular patch with coaxial probe as the feed network. Since most researchers did not fabricate their designs, the current study involves fabrication of the design.

CHAPTER THREE

MATERIALS AND METHODS

This chapter investigates the parameters used in the patch design, the design models and the fabrication method of the CMPA consisting of an outer annular ring enclosing a centrally located circular patch.

3.1 Selection of Design Materials

Ansoft HFSS is used in the designing as a 3-D Electromagnetic field solver with an engine which gives more accurate solutions using the Finite Element Model (FEM). It was used since it has a powerful post-processor which studied the electrical performance of the antenna. The effects of return loss, directivity and gain of antenna were simulated using this software. Fabrication of the antenna was done by photolithography method which involved etching out the unwanted parts. The circular patch was fed using a coaxial probe while the annular patch was an auxiliary element.

3.1.1 Selection of the Substrate

The PCB substrate selected had a fibre glass dielectric material with layers of copper on the upper and the lower parts. Its dielectric constant (ε_r) was the most important parameter in determining the performance of the MSA which is in the range of ($2.2 \leq \varepsilon_r \leq 12$). The required height (h) of the substrate is within the range of ($0.003\lambda \leq h \leq 0.05\lambda$), where λ is the wavelength. The FR4 Glass Epoxy with a dielectric constant (ε_r) of 4.4, loss tangent of $\delta = 0.02$ and a thickness/ height (h) of 1.6 mm is used as the dielectric substrate. It was selected because it is easily available in the market, had a small thickness and a high resistance to heat at a transition

temperature of 120 ^{o}c. The FR4 has a fibre glass with a density of 1.850g/cm^{3} that is flame resistant. Its structure comprises of four Bromine elements as shown in Figure 3.1:

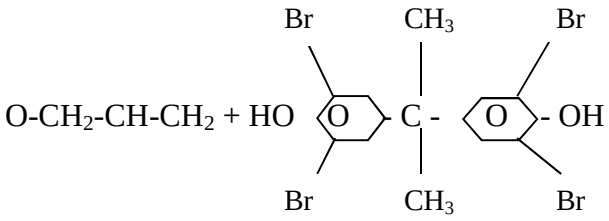

Figure 3.1: Structure of FR4 Brominated Epoxy Resin

The hydroxyl groups (-OH) provide functionality for chain extension. The same substrate was used for the CPA and the CMPA due to its high electrical insulating quality in both dry and humid areas with dielectric strength of 20 MV/m. This antenna required a lighter substrate with a smaller thickness for use in WLAN (Wireless Local Area Network) devices. The dielectric material also offers a better radiation since its permittivity has smaller value.

3.1.2 Selection of Resonant Frequency

WLANs communication frequency ranges from 2.40-2.48 GHz and 5.4 GHz. The resonant frequency (f_o) of operation selected was 2.4 GHz, a frequency commonly used in Wireless Sensor Networks (WSN) and WIFI. The radius of the circular patch and width of the annular patch were varied as the analysis was done until the frequency of 2.4 GHz was attained.

3.1.3 Selection of Feeding Techniques

The feeding technique used was coaxial probe. In the coaxial probe feed, the inner conductor of the coaxial connector extended through the dielectric to the conductor (X) while the outer

conductor was connected to the ground plane (Y) as shown in figure 3.2. Probe feed was the most preferred in this research work because it gave a low spurious radiation, The MSA was fed by applying a voltage difference between a point on the radiating element and a point on the ground conductor. The position of the feed point was done using trial and error method while moving it towards the origin. Current was maximum towards the centre of a half wave patch and zero at the end. The feed point with the lowest return loss was selected at $X_f = 4$ and $Y_f = 0$. Coaxial probe therefore became the most suitable in probing the circular patch as the reference antenna.

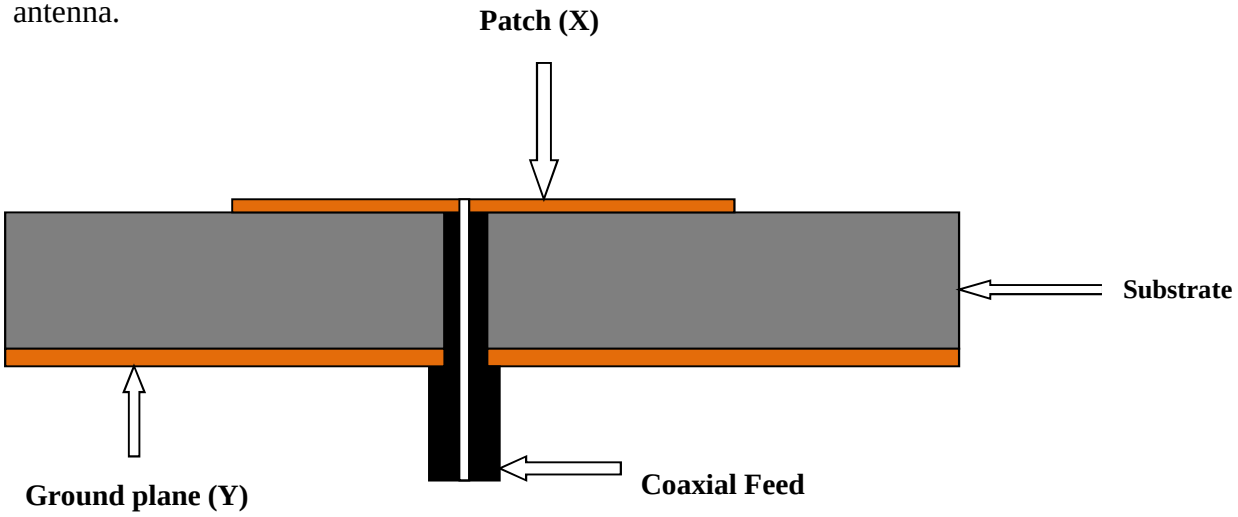

Figure 3.2: Schematic diagram of a coaxial probe

3.2 Determination of Antenna Patch Dimensions

A circular and an annular shape were used due to their reduced size compared to other shapes. The important parameters in the CMPA were the radius, a, of the antenna and the position of the coaxial probe feed on the circular patch. Figure 3.3 shows a circular patch MPA on an x-y plane with radii, a, b and c.

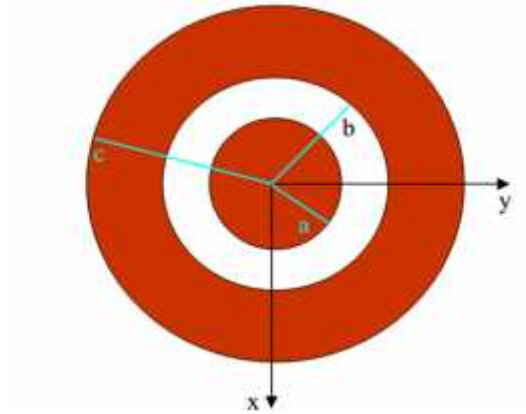

Figure 3.3: Diagram showing patch radii

3.2.1 Circular Patch Design

A circular patch also produces circularly polarized waves due to its shape. The CPA's upper surface was designed as shown in figure 3.4 where the patch has a radius, a, thickness, h and dielectric constant, ε_r.

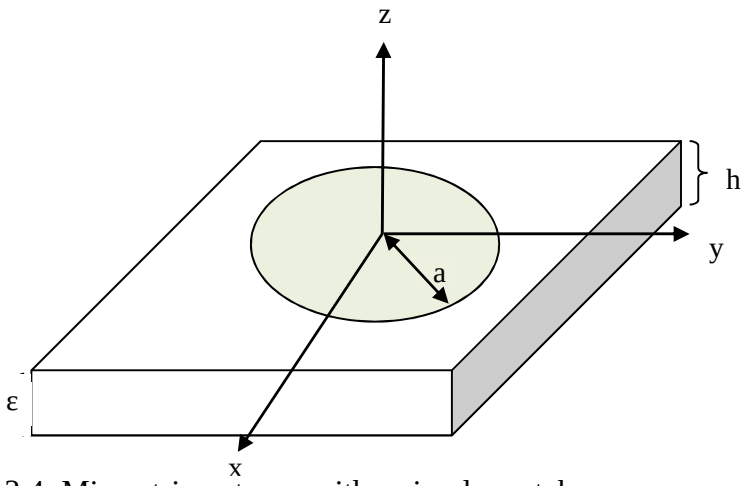

Figure 3.4: Microstrip antenna with a circular patch

The fundamental mode of a circular patch is TM_{11} from the cavity theory. The electric field, E, in the z-direction, the magnetic field, H, in the x and y-direction, are the only field components. The dimension of the circular patch was treated like a circular loop. The radius, a, from figure 3.3 was calculated from equation (3.1) and (3.2) (Kwaha *et al.*, 2011).

$$a = F\left\{1+\frac{2h}{®F£_r}\left[\ln\left(\frac{®F}{2h}\right)+1.7726\right]\right\}^{-\frac{1}{2}} \tag{3.1}$$

$$F = \frac{8.791\times10^9}{f_r\sqrt{£_r}} \tag{3.2}$$

where, f_r is the design frequency, $ε_r$ is the dielectric constant and h, is the thickness of the dielectric substrate. Considering fringing fields, the effective radius was calculated using equation (3.3) below. (Balanis, 2005)

$$a_e = a\left\{1+\frac{2h}{®a£_r}\left[\ln\left(\frac{®a}{2h}\right)+1.7726\right]\right\}^{\frac{1}{2}} \tag{3.3}$$

Fringing which occurred at the edges of the patch made the radius electrically larger (a_e = 17.46mm) than the physical radius calculated using the cavity model and microstrip patch antenna calculator. The resonant frequency of the circular disk operated at TM_{nm} dorminant mode which is TM_{11} mode using the relation given by equations (3.4) and (3.5) (Balanis, 2005).

$$X_{nm} = ka \tag{3.4}$$

$$f_{nm} = \frac{X_{nm}C}{2®a_e\sqrt{£_r}} \tag{3.5}$$

where, a_e is the effective radius, $a_e = 17.46mm$. X_{nm} is the m^{th} zero of the root of $J_n'(x)$, the derivative of Bessel's function of the first kind for non negative integers of X_{11} = 1.8412.

3.2.2 Annular Patch Design

The annular patch helps in reducing the fringing effect. The annular ring comprised of an inner circle and the outer circle. The mean circumference, C of the ring corresponded to the guided wavelength, λ_g as shown in equation (3.6). Figure 3.5 shows the top view of a circular patch with annular patch

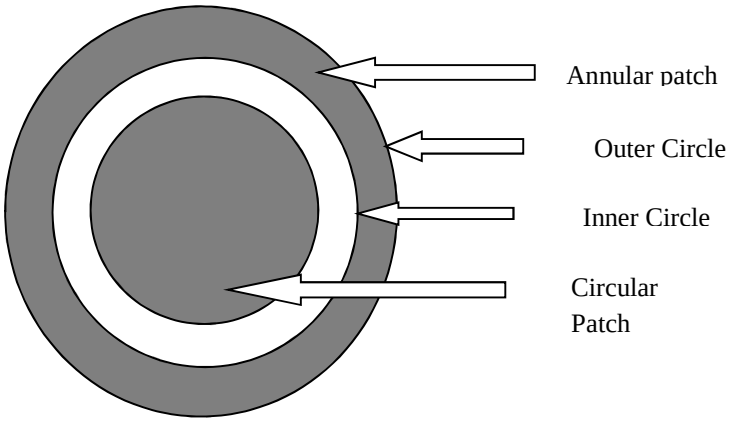

Figure 3.5: The top view of a circular with annular patch

$$C = 2\pi r = \lambda_g \tag{3.6}$$

$$\lambda_g = \frac{v}{f_r} \tag{3.7}$$

where, $\lambda_g = 125mm$, $v = 3.0\times10^8 m$, is speed of light in air and r, is radius of circle. The inner circular patch and the annular patch operate at different resonant modes. The annular ring comprises of the inner radius, b and the outer radius, c. The inner radius b, of the annular ring was calculated using TM_{12} mode because the annular patch requires a higher mode. For $TM_{nm,}$ if m is odd then there is opposite polarity between the inner and the outer fringing fields resulting to destructive interference and thus reduced radiation. If m is even then there is constructive interference resulting to good radiation mode. No fringing field was taken into account for the

annular patch since it was an auxiliary patch. Therefore equation (3.5) for resonant frequency TM_{12} mode was used in the calculation of the inner radius, b. The roots X_{nm} of modified Bessel function of the Second kind was used for the inner radius of the annular design. Where X_{12} = 2.2635. The value of b = 21.46mm. An increase in the ratio $\frac{c}{b}$ resulted to increased directivity. The resonant mode was changed using the ratio of the outer radius, c to the inner radius, b. A ratio of 2.5 was used to determine the radius of c where, c = 52.38mm. These values were used in the simulation process.

3.2.3 Feed location Design

The wireless network requires an input impedance of 50 Ohms (Ω). The feed technique was coaxial probe with an input impedance of 49.578398 Ω as shown in Figure 3.6. The alternating current circuit impedance is affected by the resistance and its reactance. Since the position of the feed was placed at any location to match the input impedance, the position of the coaxial feed was obtained by using trial and error method starting from the centre of the circular patch.

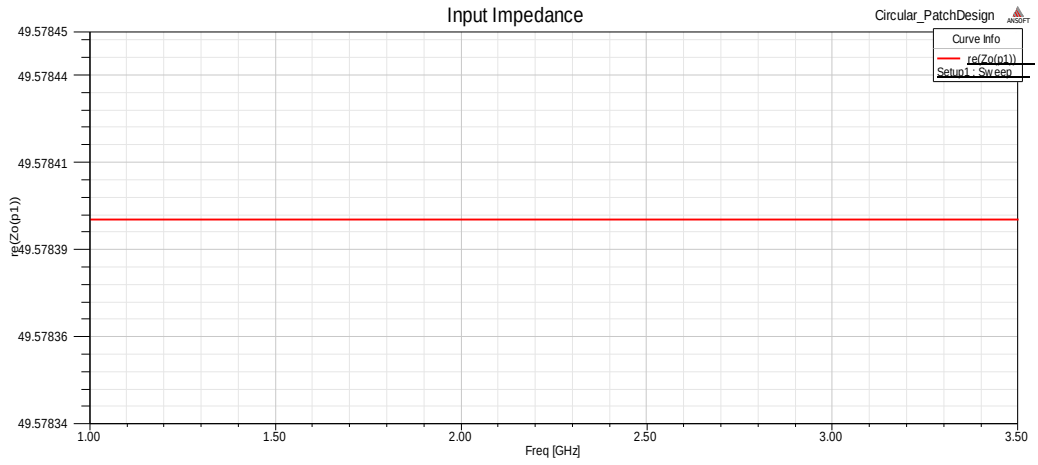

Figure 3.6: Graph of input impedence of 49.578398Ω

3.3 Modeling Design Methods

Microstrip antennas are very important due to their use and applications. The study of its physical insight involves various methods of analysis like the Cavity Model and Finite Element Method (FEM). These methods can be used in predicting some antenna characteristics like the resonant frequency, patch radius and coaxial probe position. The initial microstrip antenna design parameters were estimated using the cavity model mathematical equations while Ansoft HFSS uses the FEM.

3.3.1 Cavity Model

The cavity model gives an insight into the radiation mechanism of an antenna (Lo *et al.*, 1979). The region between the patch and the ground plane is treated as a cavity. It provides a mathematical solution for the electric and magnetic fields of a MSA. The patch and the ground plane are represented with perfect electric on top and bottom. Edges of the substrate are modelled with perfectly conducting magnetic walls. Far field and radiated power are computed from the equivalent magnetic current around the edges of the patch. A design and analysis of a circular patch MSA using different substrate was done using the cavity model (Kwaha *et al.*, 2011).

3.3.2 Finite Element Method (FEM)

FEM is used in Ansoft HFSS software for calculating the electromagnetic behaviour of a structure. FEM analyses complex structures and subdivides them into small tetrahedrons called elements, analyses then assembles them. The field in each element is approximated using a mathematical expression. FEM solves wave equations with inhomogeneous boundary conditions using Laplace equation and inhomogeneous wave equation. It can be used to define the electrical and geometrical properties of each small structured element independently. Gunel and Zoral

(2014) investigated FEM and step by step Eigen value perturbation method. They discovered that the Eigen value corresponds to the resonant mode and the results suggested that the method works well with Ansoft HFSS.

3.4 Design of the Patch Antenna

Ansoft HFSS was used in the design as a Computer Aided Design (CAD) tool which uses the Finite Element Method. The design window is fed with the different values of radius, coaxial probe position, air box size and ground plane size on the interface provided. It required drawing of 3-D Geometry, specification of parameters and the setup of the solution. The values used in Ansoft HFSS design are shown in Table 3.1. The essential parameters with fixed values used in all the design were: the resonant frequency (f_o) of 2.4GHz, dielectric constant (ε_r) of 4.4, dielecric thickness (h) of 1.6mm, air box height of 32.84mm.

Table3.1: Specification of antenna patch design.

PARAMETERS	**SPECIFICATION**
Circular Patch radius, a(mm)	16.95
Inner circle radius, b(mm)	20.93
Outer circle radius, c(mm)	52.33
Frequency (GHz)	2.4
radius of probe feed (mm)	1.6
Input Impedance (Ω)	50
Distance of feed from the centre of patch (mm)	4
Height of substrate; h (mm)	1.6
Dielectric constant of substrate (ε_r)	4.4

The design was done using Ansoft HFSS Project menu as shown in Figure 3.7.

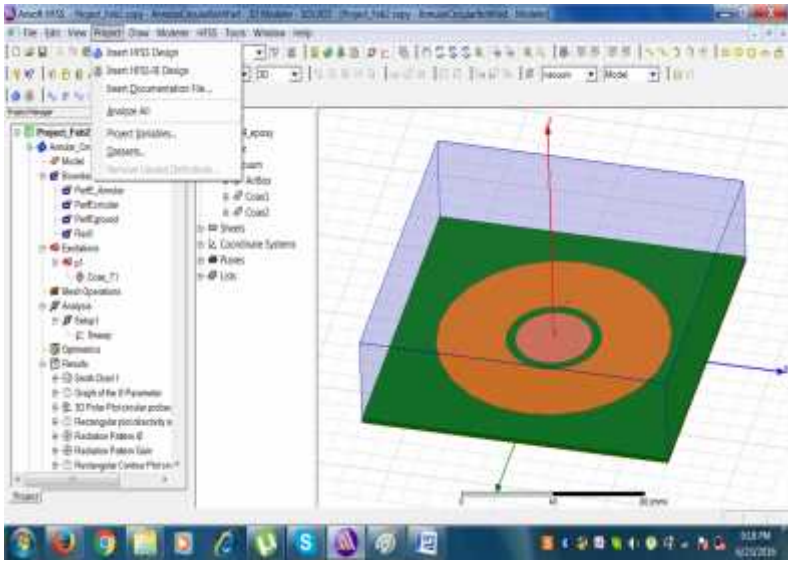

Figure 3.7: Design window of Ansoft HFSS

A new project was created in HFSS Design window. The substrate was created with the following dimensions: (dx: 120mm, dy: 110 and dz: 1.588). The circular patch was then designed with a coax pin and the air box around it.

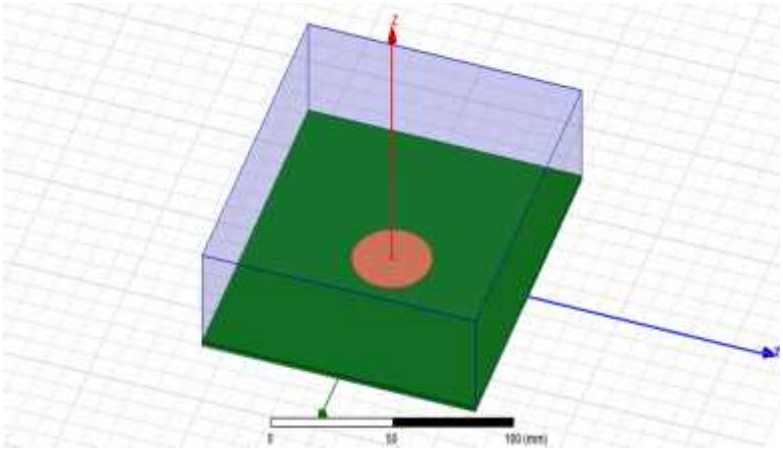

Figure 3.8: HFSS design of circular patch

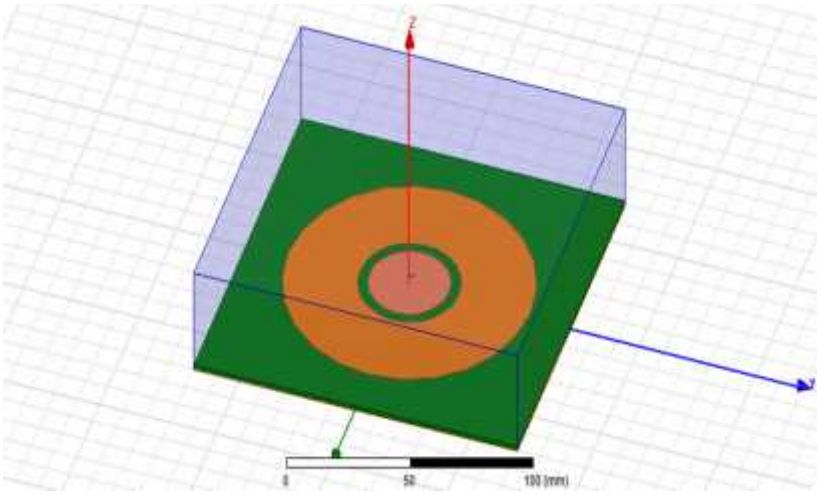

Figure 3.9: HFSS design of CMPA

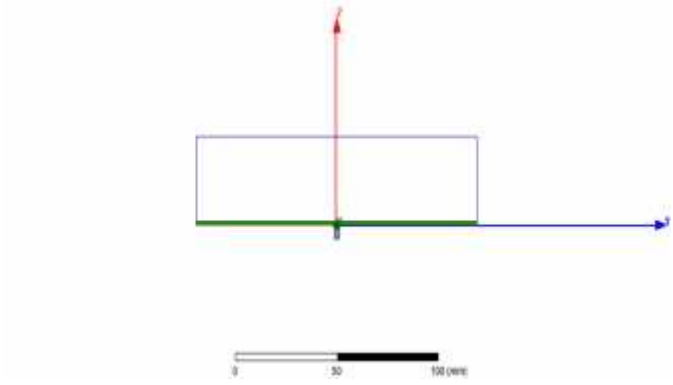

Figure 3.10: Schematic diagram of probe position

The parameters of the design stage were displayed in the antenna parameters dialogue box in

3.5 Optimization

Optimization was done to select the best radius of the circular patch and the annular patch. The effect of the change in the radius of the circular patch and change in the width of the annular patch was investigated in the simulation. The software automatically computed and generated the designs. The best result after optimization was then used in the final design. This was done by identifying a radius which could give a frequency of 2.4 GHz. Ansoft HFSS. This is displayed in the window shown in Figure 3.11. The parameters compared during the optimization are directivity, gain, return loss and polarization ratio.

3.5.1 Directivity

This is the concentration of the radiation to the direction of the maximum. Directivity is the property of radiating more strongly in one direction than others. The antenna radiation was better when the value of the directivity increases. If directivity = 0, then the antenna radiates equally in all directions. It is the ratio of the radiation intensity to the direction of maximum of the average radiation intensity. Radiation intensity is the product of the power density and the square of radial distance from the antenna.

$$Directivity = \frac{MaxRadiationIntensity}{AverageRadiationInensity}\frac{U_{\max}}{U_O} \tag{3.1}$$

3.5.2 Gain

Gain is measured in decibels (dB) and is used to compare the designed antenna's maximum radiation intensity with a standard reference antenna of the same power input. The reference antenna can be a dipole or an isotropic radiator.

Gain = directivity * efficiency

$$Gain = 10\log_{10}[directivity * efficiency]dB \tag{3.2}$$

Or

$$Gain = \frac{U_{\max}}{U_{ref}} \tag{3.3}$$

3.5.3 Return Loss (RL) or S-Parameter

It describes the input-output relationship between the ports (terminals) in an electric system. A port is any place where voltage and current can pass through. It gives a relationship of how much

power is lost relative to the incident power by the antenna. Return Loss occurs due to the mismatch load, so the lowest is required.

$$RL = 10\log_{10}\left(\frac{P_i}{P_r}\right) \text{where, } P_i \text{ is incident power and } P_r \text{ is reflected power.} \quad (3.4)$$

Return Loss measures the effectiveness of the power delivery from the transmission line to the antenna. A circular patch antenna uses the TM_{nm} mode. Therefore, S_{11} being a lower dominant mode makes a better match for the antenna and the transmission line.

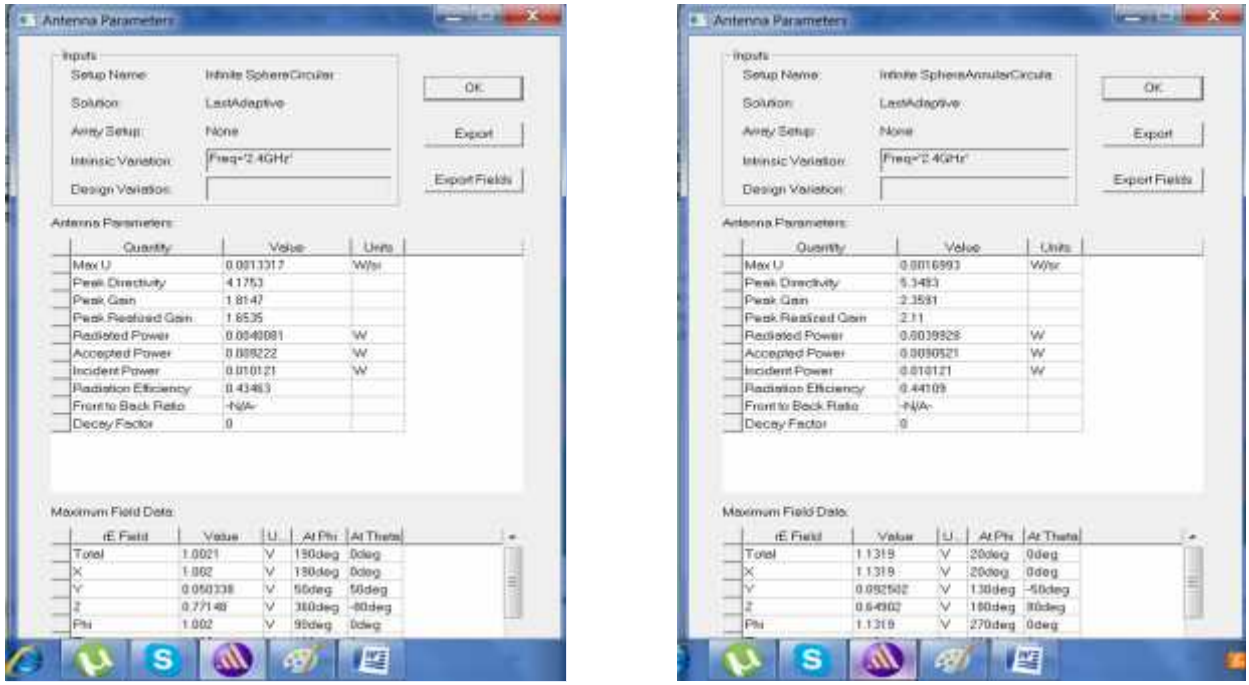

Figure 3.11: HFSS design parameters dialogue box

3.5.4 Polarization Ratio

Polarisation Ratio is the ratio of the phasors of the two orthogonal polarization components. It is a ratio between the peak level of the cross polarization radiation and the peak of the co-polarization radiation (induced radiation)

$$P.R. = \frac{E_y}{E_x} \tag{3.5}$$

3.5.5 Circular Patch Optimization

The circular designed specifications used are shown in table 3.2. The designed radius of the patch was varied to optimize for the required radiating frequency of 2.4 GHz and the results obtained displayed in table 3.2

Table 3.2: Values of parameters of radius of circular patch

RADIUS (mm)	16.90	16.95	17.00	17.05	17.10	17.15	±0.005
FREQUENCY (GHz)	2.4375	2.4250	2.4250	2.4125	2.4125	2.4000	±0.00005
PEAK DIRECTIVITY	4.1748	4.2816	4.2295	4.1493	4.1425	4.1753	±0.00005
PEAK GAIN	1.8049	1.8609	1.8396	1.8037	1.795	1.8147	±0.00005
PEAK REALIZED GAIN	1.2942	1.4487	1.5268	1.5821	1.6194	1.6535	±0.00005
RADIATED POWER (W*10^3)	3.14	3.43	3.65	3.86	3.96	4.01	±0.005
ACCEPTED POWER (W*10^3)	7.26	7.88	8.40	8.88	9.13	9.22	±0.005
INCIDENT POWER (W*10^2)	1.012	1.0121	1.0121	1.0121	1.0121	1.0121	±0.00005

3.5.6 Annular Patch Optimization

Table 3.3: Values of parameters of inner radius of the annular patch

PARAMETER						**Error**
INNER RADIUS (mm)	**20.83**	**20.93**	**21.23**	**21.31**	**21.33**	**±0.005**
FREQUENCY (GHz)	2.3725	2.3810	2.3960	2.4000	2.4025	±0.00005
PEAK DIRECTIVITY	11.167	11.431	11.545	11.569	11.469	±0.0005
PEAK GAIN	4.1702	4.3227	4.4098	4.4477	4.3996	±0.00005
PEAK REALIZED GAIN	3.7408	4.0628	4.3199	4.3726	4.3217	±0.00005
RADIATED POWER (W*10^3)	3.4	3.5963	3.79	3.83	3.81	±0.005
ACCEPTED POWER (W*10^3)	9.0787	9.51	9.92	9.95	9.94	±0.005
INCIDENT POWER (W*10^2)	0.01012	0.01012	0.01012	0.01012	0.01012	±0.00005

After optimization, the best values for the radius are used in the fabrication of the two antennas; CPA and CMPA. The values used are displayed in table 3.4.

Table 3.4: Specification values of CMPA

DESIGN PARAMETERS	
PARAMETERS	**SPECIFICATIONS**
Circular Patch radius, a(mm)	17.15
Inner circle radius, b(mm)	21.31
Outer circle radius, c(mm)	52.33
Frequency (GHz)	2.4
radius of probe feed (mm)	1.6
Input Impedance Zo (Ω)	50.00
Distance of probe feed from the centre of circular patch (mm)	4
Distance of probe feed from the centre on annular patch (mm)	24.95
Type of feed	probe
Height of substrate (h) (mm)	1.6
Relative permittivity of substrate (ε_r)	4.4

3.6 Fabricated Design

The microstrip patch antenna was fabricated by photolithography method. The method of photolithography uses a chemical process to etch out the unwanted parts of the metallic patch. Chemical etching is the process of fabricating a patch using a photo-resist, developer and etchant to remove a selected area of the patch. A design and fabrication of a half-wave rectangular microstrip patch antenna of resonant frequency 1950 MHz was done using photolithography technique with RO3003 copper clad substrate from Roger, USA and EMCoS (Electromagnetic Compatibility Software) Virtual Lab (VL) Method of Moment electromagnetic software for the simulation software (Sanjay *et al.*, 2013).

3.6.1 Fabrication Process

Photolithography uses the additive and subtractive method to produce a highly accurate etched pattern. Patterns are transferred by optical means. Any errors due to the fabrication process, changes the resonant frequency. The FR4 PCB used is shown in Figure 3.12.

Figure 3.12: Unexposed FR4 pcb

The unexposed PCB was cut into the required size and the plastic protection film carefully removed. The board was covered with a resist material that sets up when exposed to UV rays.

3.6.1.1 Photo masking stage

Computer Aided design of the antenna geometry was used in printing the transparent sheet using Express PCB software. An artwork of the design was printed as a mask on the transparent sheet.

A photo-resist is a liquid that can be applied onto a substrate, exposed with a desired pattern and developed into a selective layer for subsequent processing. A double sided copper with FR-4 dielectric Substrate was cleaned because the etched pattern's resonant frequency can be affected by dust particles. A positive UV translucent artwork was made with the printed layout of the required design.

3.6.1.2 Exposure Stage

The printed photo-resist film was laminated to the surface of the cleaned copper FR-4 substrate using a laminator and placed in an exposure unit of Ultra-Violet (UV) light using Phillips bulb TL 20W/05 (Made in Holland) for 2 minutes. The UV light transmitted through the clear part of the film and cured the photo-resist. The light irradiated on the resist interacted with it to add protons to the FR4 epoxy. The epoxy group in the resin, cross-linked to form a cured structure with a high stability to chemical and radiation damages. The UV light printed and protected the resist ink. The photo-resist used as a masking film became soluble when exposed to UV light while the unexposed parts were hardened. The transparent sheet was removed and the board taken for developing.

3.6.1.3 Developer stage

Sodium Hydroxide (NaOH) was used as a positive developer to remove the hardened photo-resist. This is a chemical dissolution of un-polymerised region. The part exposed to the UV light becomes hard and the unexposed part dissolves in the developer solution.

3.6.1.4 Etching stage

The developed copper FR-4 dielectric substrate was chemically etched out using hydrated Iron III Chloride ($FeCl_3$) solution producing a patch as shown in Figure 3.13. Ferric Chloride was preferred because it is odourless, is not absorbed by the skin and is corrosive. Ferric Chloride Solution became more acidic when broken down into its ions during hydrolysis.

Ferric Chloride = Ferric ions + Chloride Ions. Water is broken down into hydrogen ions and Hydroxyl ions.

$$H_2O \rightleftharpoons H^+ + OH \qquad (3.8)$$

Ferric ions partially combine with Hydrogen ions and Hydroxyl ions to form Ferric Hydroxide. The solution then became acidic due to an excess of hydrogen ions during precipitation.

$$Fe_2^{3+} + 3OH \longrightarrow Fe(OH)_3 \quad (3.9)$$

Since metals are electro-negative, copper then replaced Iron from the solution forming a mixture of ferrous and cupric ions.

$$2Fe^{3+} + Cu_{(s)} \rightleftharpoons 2Fe^{3+} + Cu^{2+} \quad (3.10)$$

Copper dissolved more easily because the ferrous ions became unceasingly stable in the acidic solution. Finally, the solubility limit, Cupric Chloride precipitated from a green to a blue solid.

Figure 3.13: Fabricated CMPA before cleaning

The patches were then cleaned using water and a home cleaner (acetone) to remove the unwanted residue as shown in Figure 3.14 for the CMPA and CPA respectively. The surface was then lubricated with oil to reduce the effect of oxidation on the patch surface.

Figure 3.14: Image of fabricated CMPA and circular patch after cleaning

The SMA connector probe was then soldered through the ground plane to the patch surface as shown in Figure 3.15.

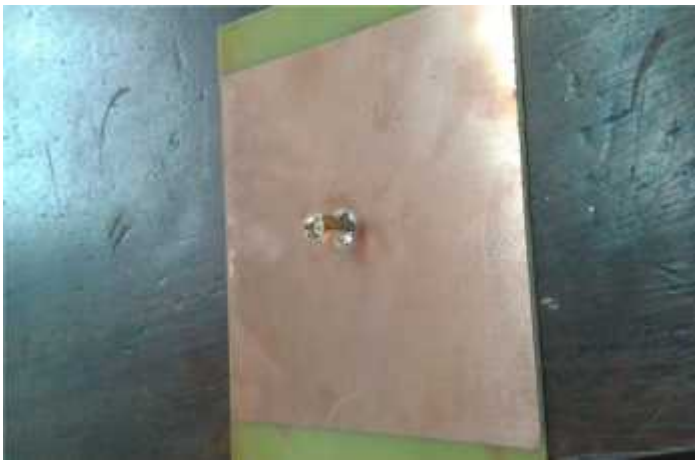

Figure 3.15: Image of SMA connector soldered on ground plane

The soldering kit used to solder the coaxial connector is shown in Figure 3.16

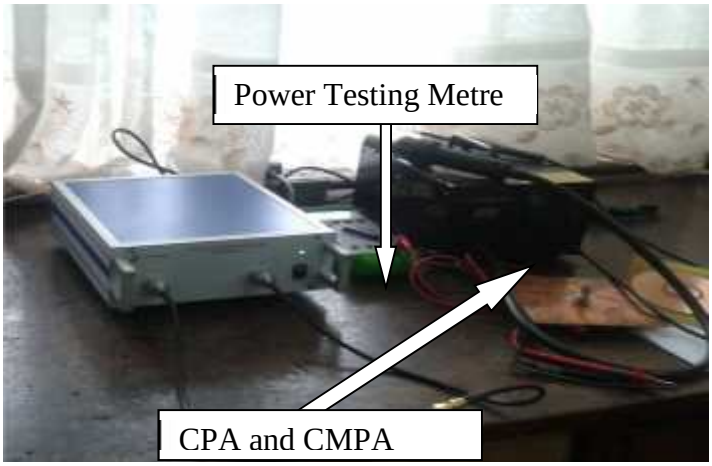

Figure 3.16: Image of soldering kit and power Tester

3.7 Selection of Testing Equipments

The Scalar Network Analyzer (SNA) shown in Figure 3.17 was used to measure network parameters like the S-parameter due to its availability. The reflection and transmission of electrical networks could easily be measured at high frequencies of between 5Hz to 1.05 THz. The SNA measured amplitude properties only. The Spectrum Analyzer was also used to study the radiated signal strength of the fabricated antenna.

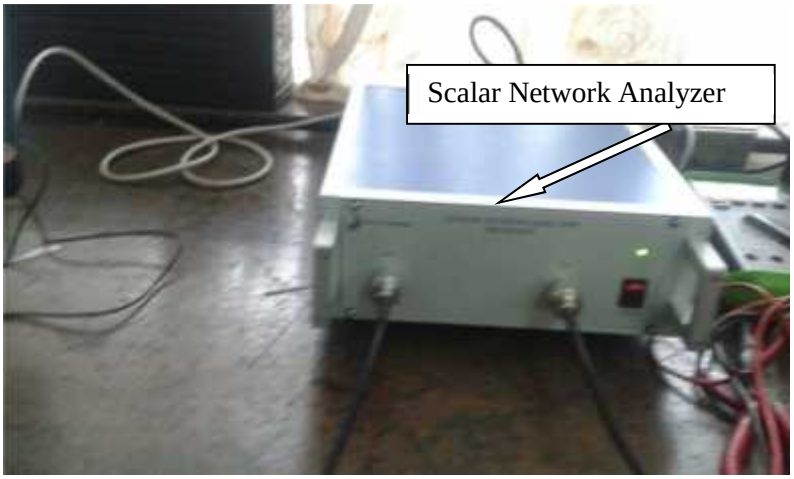

Figure: 3.17: Image of Scalar Network Analyzer

3.7.1 Initialization Process

The SNA was connected for initialization as shown in Figure 3.18. The Scalar network analyzer was given an IP Address of 192.168.0.1 for network communication as a signal generator. The analyzer was tested and reset to the required range of frequencies to be displayed on the monitor. The power Sweeps were also selected including the S_{11} transmission mode for the circular patch. The screen displayed the amplitude and phase information showing the Return Loss of the antenna at a centre frequency of 2400MHz.

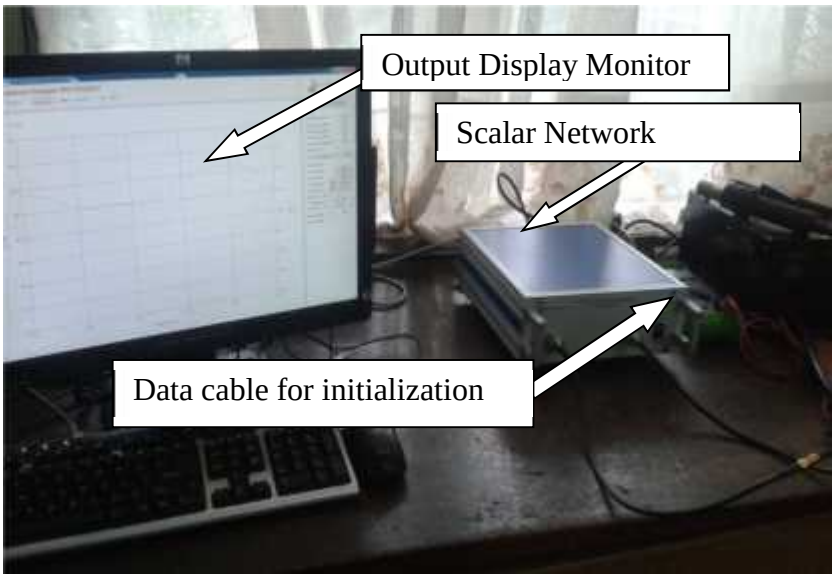

Figure 3.18: Image of initialization connection of Scalar Network Analyzer

The generated signal from the SNA was then routed to the receiving antenna which was connected to the fabricated antenna as shown in Figure 3.19 and 3.20.

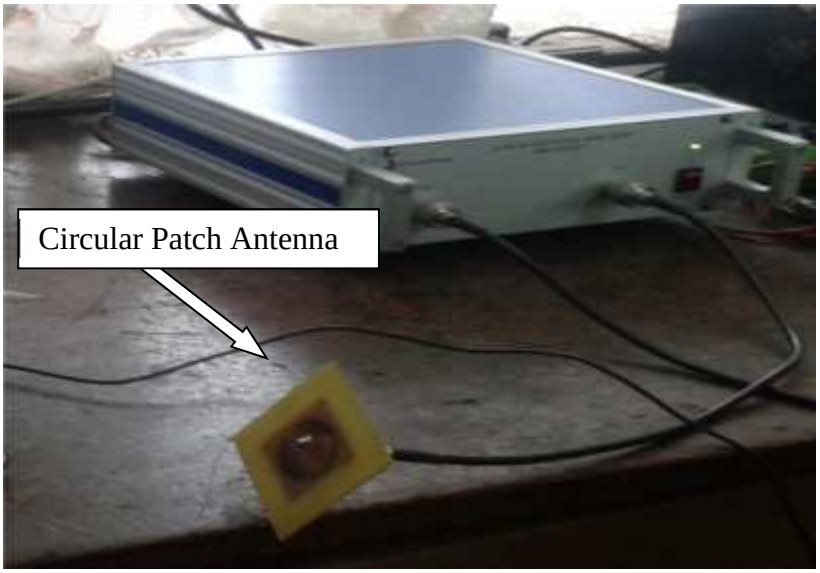

Figure 3.19: Image of circular patch antenna Testing

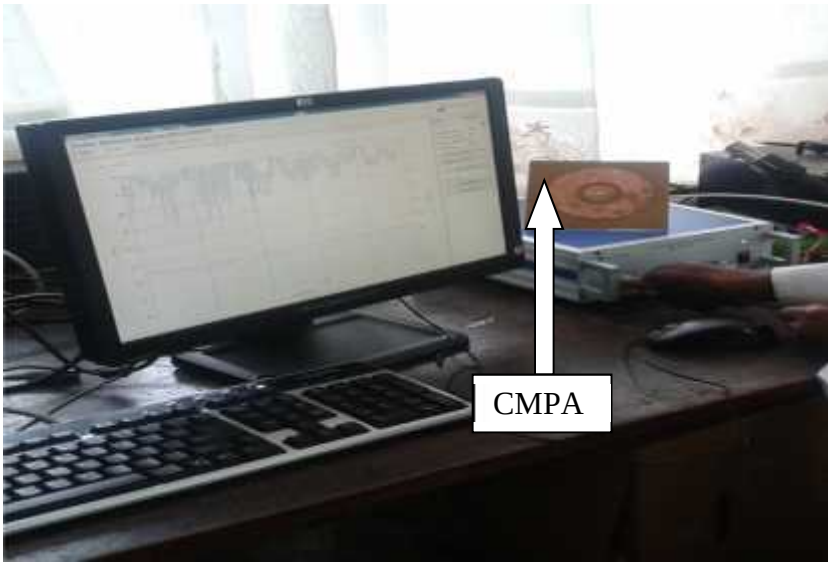

Figure 3.20: Image of CMPA Testing

The receiving antenna was connected to Port 1 and used to measure the magnitude of the signal. The signal available from the receiving antenna was processed, interpreted and displayed as a linear interpretation of the S-Parameter. A graph of the RL against frequency was displayed on monitor as shown in Figure 3.21.

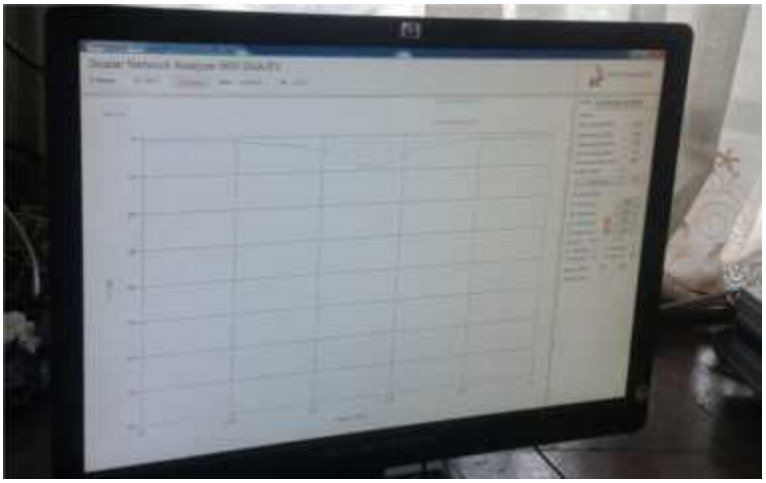

Figure 3.21: Image of S_{11} against RL Screen

3.8 Summary on materials and methods

Materials used in this study were determined by their availability. Different methods were also used to determine the parameters of the patches. The correct coaxial feed position was finally settled on after trial and error method was used. Photolithography was preferred for the fabrication process as a more accurate and available method. The testing of the fabricated antenna was done using the SNA and signal generated by the antenna monitored using a handheld spectrum analyzer and Airview software.

CHAPTER FOUR

RESULTS AND DISCUSSION

4.1 Introduction

For the design, simulation and optimization process, the results of the change in radii of the CPA and CMPA are studied using Ansoft high frequency structure simulator (HFSS). The radiation patterns, return loss, gain and directivity results are analysed in Ansoft HFSS. The testing of the fabricated CPA and CMPA is done using spectrum network analyser (SNA). The results of the return loss (RL) on the simulation and experimental antenna are compared and presented as graphs, far field patterns, tables, radiation patterns and smith charts.

4.2 Optimization results from the simulations

The parameters used in the simulated design of the antenna were studied in order to get the best patch radius radiating at 2.4GHz. Equations (3.1), (3.2), (3.3), (3.4) and (3.5) were used in calculation of the radius which was compared to the radius obtained during the simulation process. The directivity and gain of the CPA and CMPA were presented in different formats.

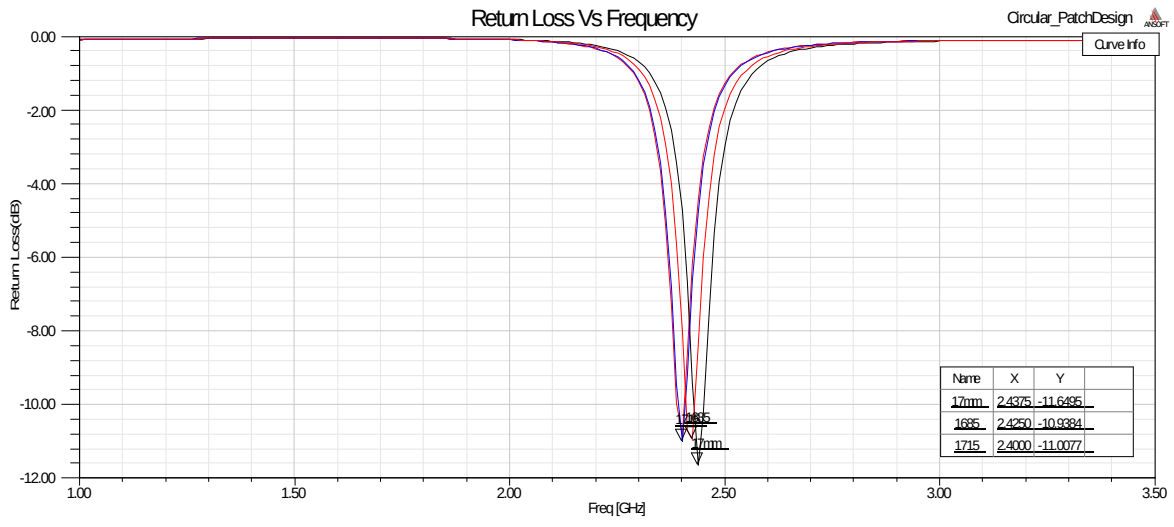

Figure 4.1: Return Loss graph with change in radius of circular patch

4.2.1 Directivity results

In the simulation, a directivity of the circular patch is 4.1753 and the Circular probe with annular patch was 5.3212 as shown in Figure 4.2.

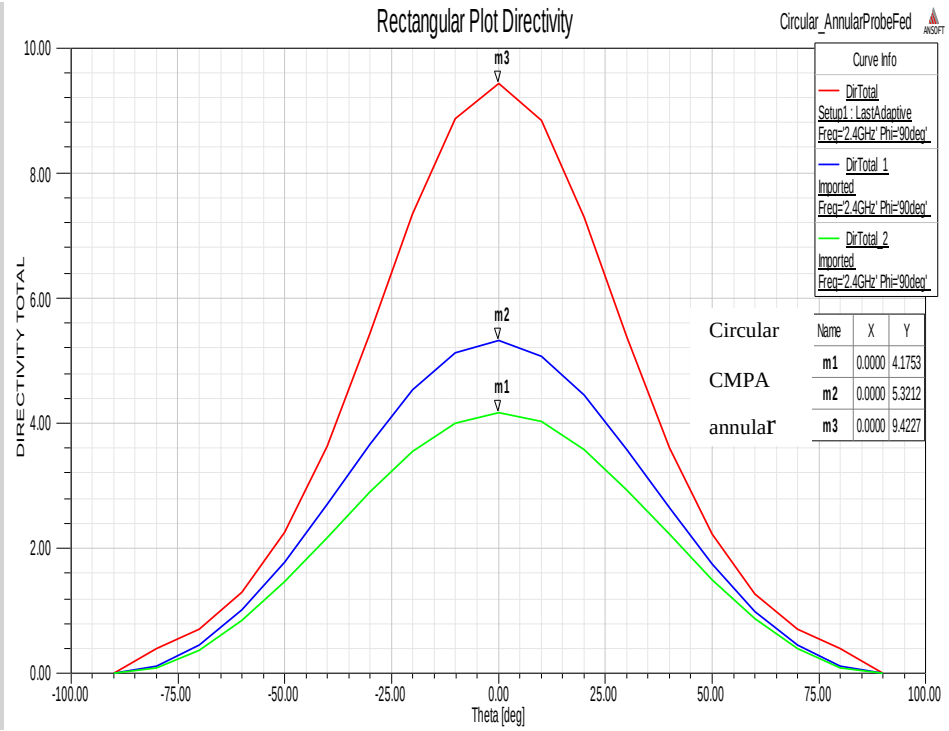

Figure 4.2: Graphs of total directivity of circular and circular with annular patch

4.2.2 Gain

The pattern obtained in the design does not have back lobes. This implies there will be reduced cross-polarization to the users. The results are shown in Figure 4.3 for circular (gain =1.817) and circular with annular (gain = 2.0964) respectively. Gain is used in amplifying the power. The broad part of a radiation pattern gives the maximum gain.

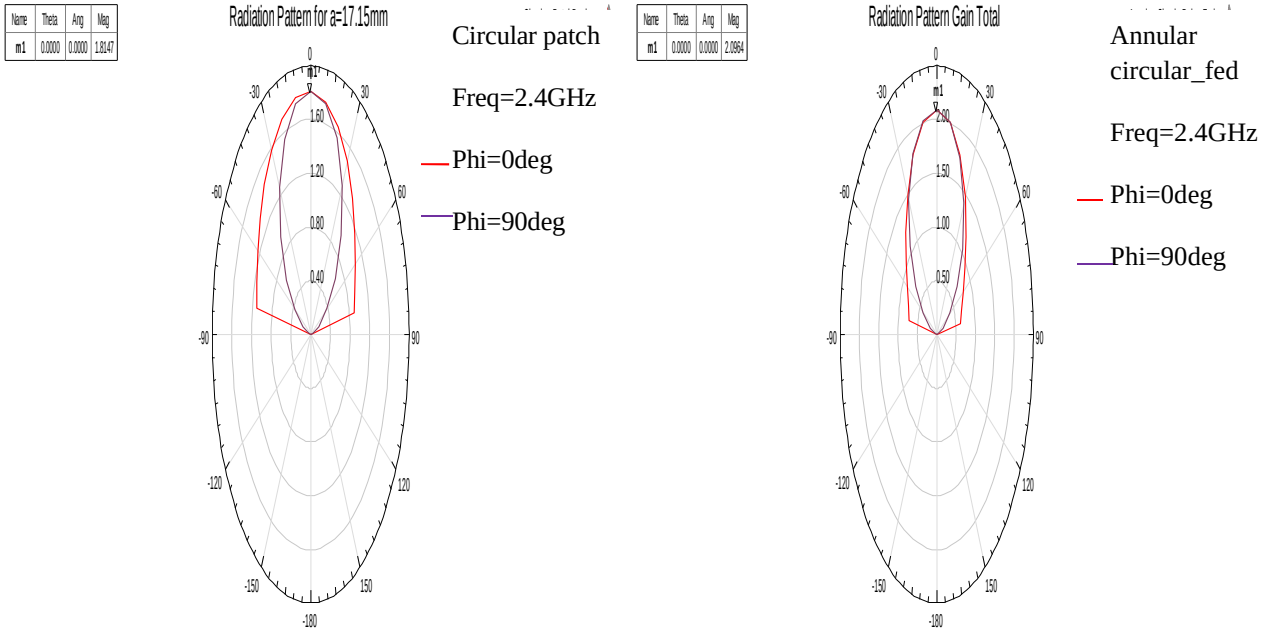

Figure 4.3: Graph of radiation patterns of circular patch at 0 and 90degrees

4.2.3 Return Loss

The best Return Loss should be lower than -10dB. The signal losses should be as low as possible. The results were obtained by varying the feed location from the centre of the patch towards the positive side of the x-axis. The coaxial probe used had a radius of 0.5mm and could handle a frequency range between 2.2 -2.6 GHz. Using the selected feed point, a RL= -9.7739dB for the circular patch of radius = 17.15mm and -10.8173 dB was attained at 2.4 GHz as shown in Figure 4.4.

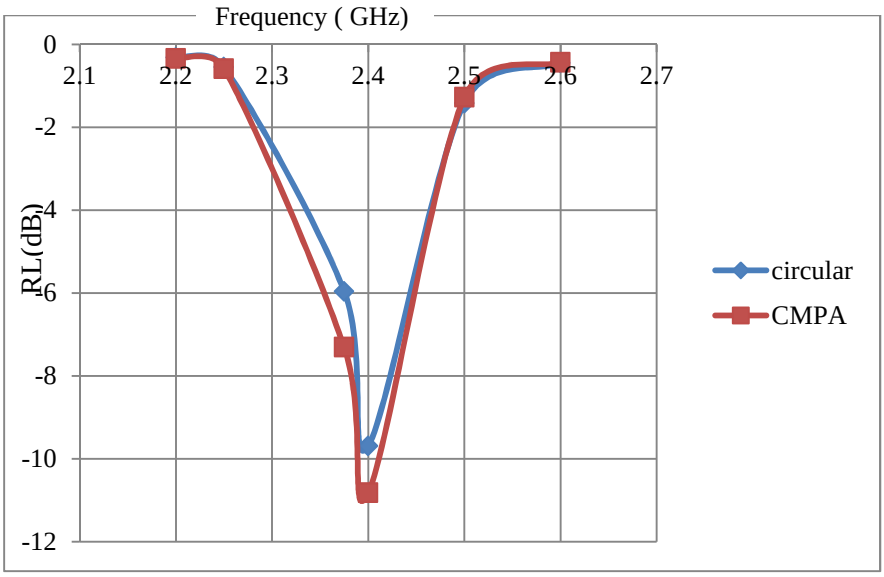

Figure 4.4: Graph of RL Vs frequency of the Circular and CMPA antenna

4.2.4 Voltage Standing Wave Ratio (VSWR)

When power is injected in the antenna, some of it is reflected back. Therefore, VSWR is the measure of impedance mismatch. This ratio should be less than 2 for a working antenna. A VSWR of 1.9611 was obtained for the Circular patch with annular patch while a VSWR of 1.8083 for the circular patch at a 2.4 GHz.

4.2.5 Far Field Pattern

It shows how good the antenna radiates in the far-field region for different angles from the antenna's position. Figure 4.5 gives the results obtained from Ansoft HFSS, where; red-antenna radiates with high power, yellow- Antenna radiates with lower power and blue-antenna radiates with no power.

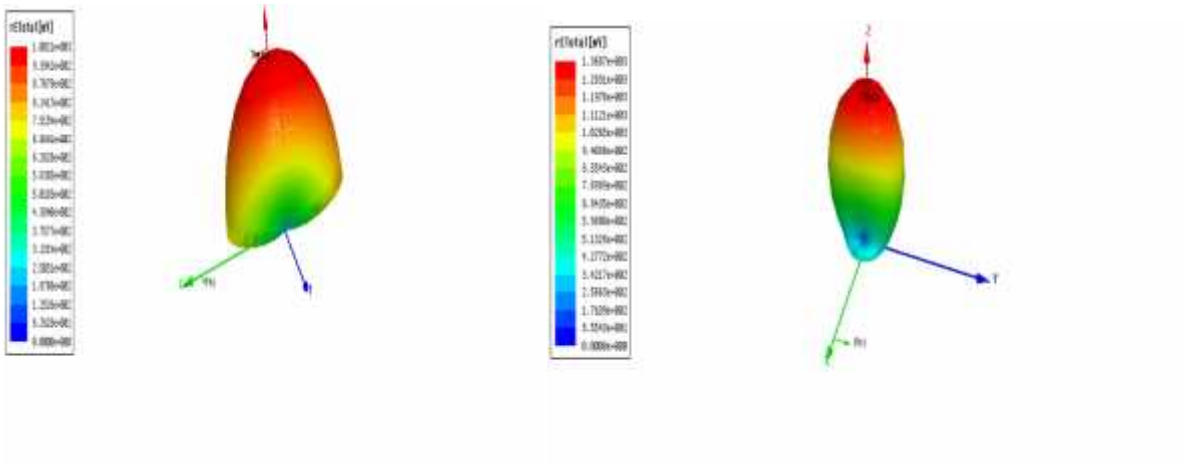

Figure 4.5: 3-D polar plot of CPA (1.002.1eV) and CMPA(1368.7eV)

4.2.6 Radiation Pattern Plots

Radiation pattern is the graphical representation of the maximum radiated power in a particular direction. A microstrip antenna radiates normal to the surface of the patch. The elevation patterns were considered in for ¤ = 0^o and ¤ = 90^o. Radiation pattern plots were used to define how the antenna radiates as shown in figure 4.6. The circular patch directivity obtained in the broad side was 4.1753 while the circularly probed patch with annular patch around it had a directivity of 5.3212. There were no back lobes observed in this antenna thus reducing the cross polarization.

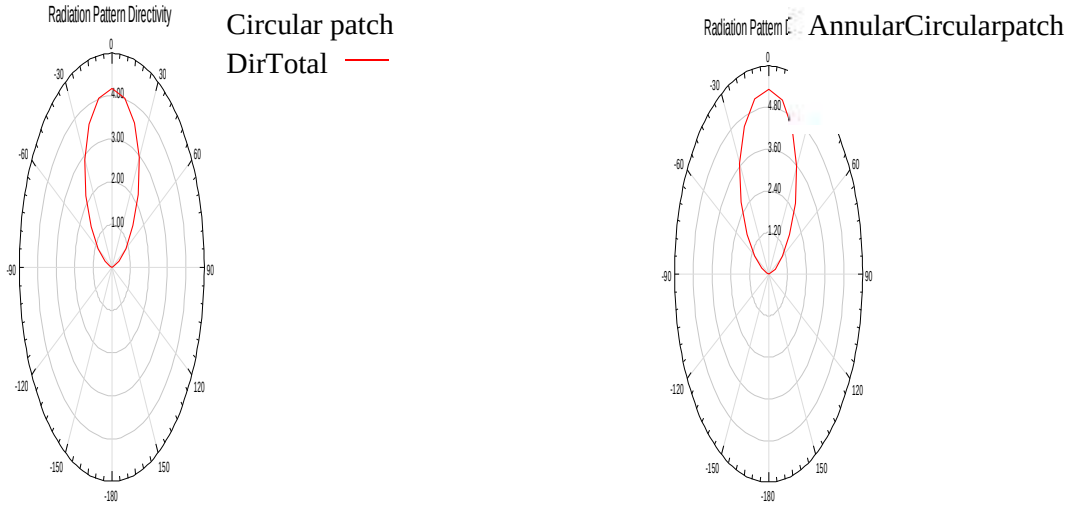

Figure 4.6: 2-D polar plot Radiation pattern at $\phi = 90^0$

4.2.7 Polarization Ratio

A system's power loss due to polarization mismatch between co-polarized and cross-polarized signals should be greater than 1. The polarization ratio of the simulations are shown in figure 4.7.

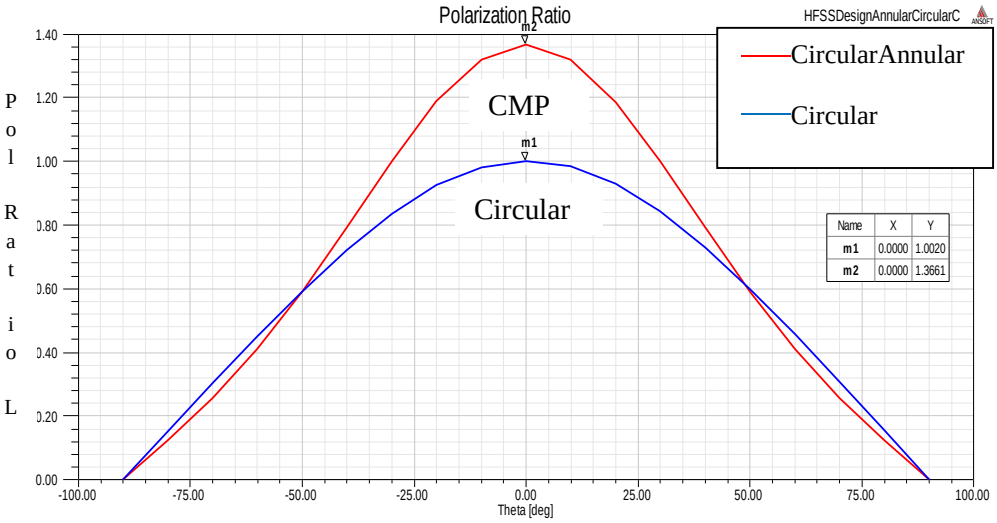

Figure 4.7: Polarization ratio graphs

4.2.8 Smith Chart

The smith chart shows how good the antenna is matched. It is a visualizing tool used to study the impedance of the transmission lines as a function of frequency. If the red line on the smith chart goes through point 1 at the horizontal line, then the reflection coefficient (Γ) is zero. At this point no power is reflected by the antenna. If the magnitude of the reflection coefficient ($|\Gamma| = 1$), then all the power is reflected. The results obtained in the simulation indicated the red line at 0.50 showing a small amount of reflection as shown in figure 4.8.

Circular patch Circular with annular patch

Figure 4.8: Smith chart of circular patch

4.2.9 Radiation efficiency

This is the ratio between the radiated power and the input power. A radiation efficiency value should be 1. Any value less than 1 confirms some losses in the radiations during transmission.

$$RadiationEfficiency = \frac{AntennaPower}{AcceptedPower} \tag{4.4}$$

The radiation efficiency of the circular patch was 0.43 and circular with annular was 0.44. Some radiation loses were experienced from these results as shown in table 4.1.

Table 4.1: Ansoft hfss simulation design parameters

Parameter	**Circular Patch**	**Circular with Annular**
Peak Directivity	4.1753	5.3483
Peak Gain	1.8147	2.3591
Radiation Efficiency	43.5%	44.1%

Table 4.2: Percentage difference in initial and designed radius after optimization

Quantity	Initial radius (mm)	Designed radius(mm)	Radius difference (%)
Circular Patch	17.46	17.15	-1.81
Annular Inner Circle	21.26	21.31	+0.70
Annular Outer Circle	52.38	52.33	-0.10

4.3 Results of the Fabrication process

The optimization of the designed patches resulted to the design with the required frequency. These designs were fabricated successfully as shown in the figures 4.9.

Figure 4.9: Image of CMPA and CPA after fabrication process

4.4 Testing of Fabricated Antenna

The testing was done using a Scalar Network Analyzer (SNA). The SNA comprises of the Signal generator, Test Set, Receiver and the Display unit. The SNA had a built-in signal generator which generated a signal for the required frequency of 2.4 GHz after initialization. A handheld spectrum analyzer generating a 2.4GHz signal was used in testing the working of the CMPA. The CMPA received signals transmitted within the range of 2.1-2.5 GHz. The strongest signal power was 2412 MHz. The noise flow was -98 dBm and bandwidth of 10MHz.

4.4.1 Results of Experimental Data

Figure 4.10 shows the graph of the S-parameter of Return loss of the fabricated CPA and CMPA respectively.

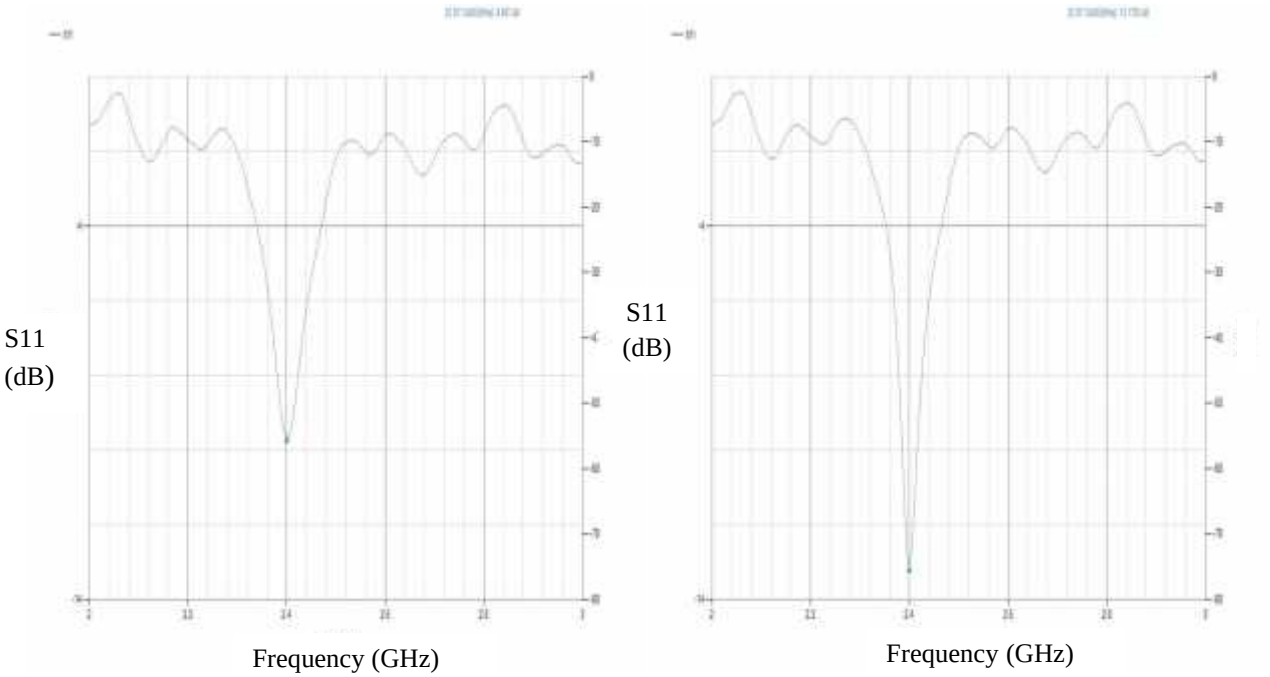

Circular patch RL= -9.6dB Circular with annular RL= -13.17dB

Figure 4.10: Graph of experimental return loss (RL)

The annular patch around the CMPA improved the performance of the circular patch antenna and the transmission loss got lowered by 35%.

4.4.2 Comparison of Simulated CMPA and Experimental CMPA

Table 4.3: Results on simulation of patches.

Parameter	Circular	Annular	Probe circular	Probe annular	Probe Both
Frequency (GHz)	2.4	2.4	2.4	2.4	2.4
Return Loss (dB)	-9.8	-18.4	-10.8	-26.7	-10.2
Peak Directivity	4.1753	11.5690	5.3825	9.4227	10.517
Peak Gain	1.8147	4.4477	2.385	3.299	3.4109

Table 4.4: Comparison of simulated data of circular and CMPA

PARAMETER	Circular	Circular with annular patch
FREQUENCY (GHz)	2.4GHz	2.4 GHz
PEAK DIRECTIVITY	4.1753	5.3483
PEAK GAIN	1.8147	2.3591
PEAK REALIZED GAIN	1.6535	2.1100
RADIATED POWER (W*10^3)	0.0040081	0.0039928
ACCEPTED POWER (W*10^3)	0.009222	0.0090521
INCIDENT POWER (W*10^2)	0.010121	0.010121
RADIATION EFFECIENCY	0.43463	0.44109

4.5 Results Analysis

The radius of the circular patch was found to be inversely proportional to the resonant frequency and directivity but directly proportional to return loss and gain. The directivity improved by 27.08%, gain by 25.86% and return loss by 45.09%. Cross polarization could not be completely eliminated. The CMPA's performance proved to be better due to its Return Loss values as compared to the circular patch antenna in both simulation and experimental results on return loss. This confirmed reduction in multipath signals by the CMPA.

CHAPTER FIVE

CONCLUSIONS AND RECOMMENDATIONS

5 .1 CONCLUSIONS

The patch antenna's radius was calculated using Ansoft HFSS which applies FEM. It also allowed for higher order modes to be used for the annular patch. The antenna's patch radius could be easily changed starting from 16.95mm to attain the required frequency of 2.4GHz at a radius of 17.15mm in the optimization stage. The radiation efficiency of the circular patch antenna was 43.5% and circular patch with annular was 44.1%. A higher directivity experienced resulted to the radiated signals affected by reflection within the same direction. During the testing process calibration errors were checked and passed.

From the results of the study, it was deduced that an increase in the radius of circular patch decreased the resonant frequency. An increase in annular-inner radius of the annular patch caused an increase in the gap, frequency and directivity. From the observations made, a circular patch was studied on FR-4 substrate and its cross polarization effect compared to a circular patch with an annular patch around it. The directivity of the CMPA was 5.3212dB from CPA directivity of 4.1753dB. The CMPA antenna is easy to fabricate and works well in the range of frequencies of wireless networks with reduced cross-polarisation. An annular ring with circular patch probe-fed improved directivity by 22.43%. A circular patch with annular probe-feed improved RL by 31.09%. Feeding both improved annular with circular-fed RL by 4.39% and directivity by 48.82%. Multiple frequencies were realised with the introduction of an annular patch around the circular patch. The directivity of the antenna improved with the introduction of the annular patch showing a reduced cross polarization. The obtained bandwidth of 0.2GHz is within the range required for wireless systems. The HFSS analysis of the circular and circular

with annular patch showed that the circular with annular patch had a higher radiation efficiency, directivity and gain. In the fabrication process, an annular patch placed around a circular patch reduced the cross polarization effect. The designed antenna is fabricated using photolithography method. The return loss results obtained after testing using SNA improved by 35.8%. The simulation RL and experimental RL improved by 21.8 %. The annular patch therefore reduces production of multipath signals. The circular patch easily contributed to circular polarization. The antenna was more stable in radiating signals due to the use of FR4 substrate as a dielectric material. Earlier studies also indicated that a circular patch was good in circular polarization using other dielectric material. Some studies also concentrated on other range of frequencies but not 2.4 GHz. Their directivity was much lower value as compared to the one studied.

5.2 RECOMMENDATIONS

This study shows that the circular patch produces circularly polarized radiations with reduced cross polarization effects. The annular patch acts as a reflector antenna to reduce cross polarization and reduce signal losses as shown by the lowered return loss value. Therefore, this study shows an improvement in the antenna efficiency with the introduction of the annular patch. In view of these, a smaller sized patch antenna that fits well in modern handheld devices is highly recommended. With availability of the right spectrum analyzer, it would be of great value to determine the power of the signal generated by the CMPA.

It was noted that the annular patch reduces cross polarization and the antenna size depending on the dielectric used; therefore, investigations can be done to determine the use of a cheaper dielectric with reduced transmission errors.

REFERENCES

Balanis, C. A. (2005). *Antenna Theory Analysis and Design*. Third Edition. New Jersey: John Wiley & Sons Inc.

Bao, X. L. and Ammann, M. J. (2006). Compact Annular-ring Embedded Circular Patch Antenna with a Cross Slot Ground plane for Circular Polarization. *Electronic Letter* **42**: 192-193.

Chattopadhyay, S. and Chakraborty, S. (2018). A Physical Insight Into the Influence of Dominant Mode of Rectangular Microstrip Antenna on its Cross-polarization characteristics and its Improvement with T-Shape Microstrip Antenna. *Institute of Electrical and Electronic Engineering Transactions on Antennas and Propagation.* **6**: 3594-3602.

Chen, H. T. and Wong, K-L. (2007). Cross Polarization of a Probe-fed Spherical-Circular Microstrip Patch Antenna. *Microwave and Optical Technology Letters* ***6***: 705-710.

Deschamps, G. A. (1953). Microstrip Microwave Antenna. *In the Proceedings of the 3rd United States Air Force Symposium on Antennas*. Monticello, Illinois, USA.

Dross, G., Wu, Z. and Davis, L. E. (1997). A Comparative Study of Circular Microstrip and Cylindrical Dielectric Resonator Antennas. *In the proceedings of the 10th International Conference on Antennas and Propagation* **436**: 38-42.

Edling T. (2012). *Design of Circularly Polarized Dual Band Patch Antenna.* Amnesgranskare: Anders, Rydberg, ISSN: 1654-7616, UPTEC E11008

Gunel, S. and Zoral, Y. (2014). Vector Finite Elements and the Step by Step Eigenvalue Perturbation Methods. *Journal of Physics*. **490**(1): 1742-6596.

Gupta, K., Jain, K. and Singh P. (2014). Analysis and Design of Circular Patch Antenna at 5.8GHz. *International Journal of Computer Science and Information Technology.* ***5***(3): 3895-3898.

Hansen, R. (1987). Cross Polarization of Microstrip Patch Antennas. *Institute of Electrical and Electronic Engineering Transactions on Antennas and Propagation 35***,** 731-732, Tarzana, USA.

Hiroyuki, M. and Yingcheng, D. (2011). *Radio Wave Antennas Antennas Microstrip.* Harada Industry of America Inc., Michigan, USA.

Howell, J. Q. (1974). Microstrip Antennas. *Institute of Electrical and Electronic Engineers Transactions on Antennas and Propagation* ***23***: 90-93.

Huang, Y. and Boyle, K. (2008). *Antennas, From Theory to Practice*. Eighth Edition. United Kingdom: John Wiley and Sons Ltd.

Https://en.wikipedia.org/Network_analyzer Accessed on 5th January 2017

Ingale, T. and Trikolikar, A. A. (2015). Simulation of Rectangular Microstrip Patch Antenna. *International Journal of Innovative Research in Science, Engineering and Technology*. ***4***(1): 18886-18891.

James, J. R. and Hall, P. S. (1989). *Handbook of Microstrip Antennas*. Wiltshire, UK: Peter Peregrines Ltd.

Kamal, E. M., Setyawati, O. and Muladi, M. (2014). Circularly Polarized MicrostripAntenna with a Frequency of 1.9 GHz-2.5 GHz for Wireless Applications. *Journal of Electronics and Communication Engineering*. ISSN: 2278-2834, **9**(1): 16-20. Retrieved from www.iosrjournals.org.

Kerr, J. L. (1978). Terminated Microstrip Antenna. *In the proceedings of the Antenna applications symposium*, Allerton Park.

Konditi, D. B. O. and Rop, K. V. (2012). Performance Analysis of a Microstrip Patch Antenna on Different Dielectric Substrates. *Innovative Systems Design and Engineering*. ***3***: 7-14.

Kumar, P., Thakur, N. I. And Sanghi, A. (2013). Microstrip Patch Antenna for 2.4 GHz Wireleess Applications. *International Journal of Engineering Trends and Technology.* **4**(8): 3544-3547.

Kwaha, B. J., Inyang, O. N. and Amalu, P. (2011). The Circular Microstrip Patch Antenna – Design and Implementation. *International Journal of Research and Review in Applied Sciences*, **8**: 86-95.

Lavado, E. N. (2009) Design of a Dual band Circularly Polarized Antenna for a Galileo Demonstrator. Theory and Literature Survey on Microstrip Antenna. Deutches Zentrum. **2**: 8-34.

Lo, Y. T., Solomon, D. and Richards, W. F. (1979). An Improved Theory for Microstrip Antennas and Applications. *In the proceedings of Antenna and Propagation Society International Symposium* **17**: 113-116.

Majumder, A. (2013). Rectangular Microstrip Patch Antenna using Coaxial Probe Feeding Technique to Operate in S-Band. *International Journal of Engineering Trends and Technology*, West Tripura, India. **4**: 1206-1210.

Marwa, S., Hammad, H. and Sebak A. (2010). Circularly Polarized Microstrip Antenna. *In the proceedings of the IEEE Middle East Conference for Antenna Propagaton (MECAP)*, Montreal, Quebec, Canada.

Mom, J. M., Roy, A. A. and Kureve, D. T. (2013). Investigation of the Effect of Feed Variation on the Performance of a Circular Patch Microstrip Antenna. *International Journal of Applied Information Systems*, New York, USA. **6:** 2249-0868

Munson, R. E. (1974). Conformed Microstrip Antennas and Microstrip Phased Arrays. *Institute of Electrical and Electronic Engineering Transactions on Antennas and Propagation*. **22**: 74-78.

Mutiara, A. B., Refianti, R. and Rashmansyah, (2011). Design of Microstrip Antenna for Wireless Communication at 2.4GHz. *Journal of Theoretical and Applied Information Technology*, Depok,Indonesia. **33**: 1992-8645

Nascimento, D. C. and Lacava, J. C. (2011). Design of Low-Cost Probe-Fed Microstrip Antennas, Microstrip Antennas. Prof. Nasimuddin Nasimuddin Ed. ISBN:978-953-307-247-0, Intech. Retrieved from http://www.intechopen.com/books/microstrip-antennas/design-of-low-cost-probe-fed-microstrip-antennas

Parker, G. S. (1997). *A Dual Polarized Microstrip Ring Antenna with Very Good Isolation*. Kingston, Ontario.

Pawar, U. A., Mondal, D., Nagaraju, A., Chakraborty S., Singh, L. L. K. and Chattopadhyay, S. (2018). Rectangular Microstrip Antenna with Corrugation Defects at Radiating edge: A new Approach to Reduce Cross Polarization. *In the proceedings of the IOP Conference on Material Science*, **331**. India.

Puthanial, M., Kishore, Raja P. C. (2016). Comparative Performance Analysis of Microstrip Patch Antenna at 2.4 GHz and 18GHz using AN-SOF Professional.In: Suresh L., Panigrahi B. (eds) *Proceedings of the International Conference on Soft Computing Systems.* Advances in Intelligent Systems and Computing, **398.** Springer, New Delhi

Ramesh, G., Prakash, B., Inder, B. and Apisak, I. (2001). *Microstrip Antenna Design Handbook.* Boston, London: Artech House.

Rao, R. B., Smolinski, M. A., Quach, C. C. and Rosario, E. N. (2003). Triple Band GPS Trap-Loaded Inverted L Antenna Array. MITRE Corporation, Massachusettes. *Microwave and Optical Technology Letters* **38:** 35-37.

Rao, R. B., Elloian, J. M., Rosario, E. N. and Davis, R. J. (2012). Ferrite Loaded UHF Sleeve Monopole Integrated with a GPS Patch for a Handset. MITRE Corporation, Bedford. *Microwave Optical Technology Letter* **54**: 2513-2516.

Sanjay, M. Palhade, and Yawale, S. P. (2013). Design and PhotoLithographic Fabrication of Microstrip Patch Antenna. *International Journal of Science and Research* (IJSR). ISSN 2319-7064.

Sharma, P., Tripathi, T. and Singh, D. (2012). Effect of Change in Dimensions of the Circular Antenna and Feedpoint on The Antenna Performance. *Global Journal of Researches in Engineering*, USA. ISSN **12**: 2249-4596.

Singh, A. and Gupta, R. K. (2014). Enhancement of Gain of Circularly polarized Microstrip Antenna using RIS and Parasitic Patches, *International Journal of Innovative Science Engineering and Technology*. **1**: 2348-7968

Singh, P., Dhubkarya, D. C. and Aggrawal, A. (2013). Design and Analysis of Annular Ring Slot Microstrip Antenna for a Wireless and UHF Applications. *In the Proceedings of the Conference on Advances in Communication and Control Systems*, Atlantis Press. 541-544

Tecpoyotl-Torres, M., Vera-Dimas, J. G. and Ruiz, R. C. (2012). Antenna Array of Adjustable Bandwidth based on Rings containing Microstrip Antennas. *Mexican Journal of Scientific Research.* **1:** 10-23

Wang, D., Song, L., Zhou, H. and Zhang Z. (2012). A Compact Annular Ring Microstrip Antenna for WSN Applications. Retrieved from nlm.ncbi.www.nih.gov

APPENDIX